Vol 15 No 5, May 2006
1009-1963/2006/15(05)/1060-07

Chinese Physics

© 2006 Chin. Phys. Soc.
and IOP Publishing Ltd

Effects of donor density and temperature on electron systems in AlGaN/AlN/GaN and AlGaN/GaN structures*

Zhang Jin-Feng(张金凤)†, Wang Chong(王 冲),
Zhang Jin-Cheng(张进城), and Hao Yue(郝 跃)

Key Lab of Ministry of Education for Wide Band-Gap Semiconductor Materials and Devices, Microelectronics Institute, Xidian University, Xi'an 710071, China

(Received 10 June 2005; revised manuscript received 19 February 2006)

It was reported by Shen *et al* that the two-dimensional electron gas (2DEG) in an AlGaN/AlN/GaN structure showed high density and improved mobility compared with an AlGaN/GaN structure, but the potential of the AlGaN/AlN/GaN structure needs further exploration. By the self-consistent solving of one-dimensional Schrödinger–Poisson equations, theoretical investigation is carried out about the effects of donor density (0–$1\times10^{19}\,\mathrm{cm}^{-3}$) and temperature (50–500 K) on the electron systems in the AlGaN/AlN/GaN and AlGaN/GaN structures. It is found that in the former structure, since the effective ΔE_{c} is larger, the efficiency with which the 2DEG absorbs the electrons originating from donor ionization is higher, the resistance to parallel conduction is stronger, and the deterioration of 2DEG mobility is slower as the donor density rises. When temperature rises, the three-dimensional properties of the whole electron system become prominent for both of the structures, but the stability of 2DEG is higher in the former structure, which is also ascribed to the larger effective ΔE_{c}. The Capacitance–Voltage ($C-V$) carrier density profiles at different temperatures are measured for two Schottky diodes on the considered heterostructure samples separately, showing obviously different 2DEG densities. And the temperature-dependent tendency of the experimental curves agrees well with our calculations.

Keywords: AlGaN/AlN/GaN, AlGaN/GaN, two-dimensional electron gas, $C-V$ carrier density profile

PACC: 7280E, 7360L

1. Introduction

The strong polarization effects in nitride-based heterostructures can modulate their energy bands and carrier distributions significantly, and result in a two-dimensional electron gas (2DEG) with the density much higher than that of conventional GaAs-based heterostructures. Shen *et al*[1] reported that AlGaN/AlN/GaN structure was superior to AlGaN/GaN structure since in the former both electron density and mobility of 2DEG were improved. The same research group in UCSB also observed experimentally the dependences of 2DEG mobility and sheet density on aluminium content and thickness of the AlGaN layer in the AlGaN/AlN/GaN structures.[2]

The wide application of nitride-based heterostructures requires not only high density but also high stability of 2DEG. So it is very important to investigate the effects of donor density and temperature on the electron systems in nitride-based heterostructures. In this paper, such investigations are carried out theoretically by the self-consistent solving of one-dimensional coupled Schrödinger–Poisson equations for the AlGaN/GaN and AlGaN/AlN/GaN structures, and the different 2DEG stabilities are compared. Meanwhile, the temperature-dependent carrier density profiles measured by the Schottky $C-V$ characteristics strongly support our calculations of the effect of temperature.

2. Model

Along the longitudinal direction the quantum

*Project supported by the State Key Development Program for Basic Research of China (Grant No 2002CB311904).
†Corresponding author. E-mail: jfzhang@xidian.edu.cn

confinement of conduction band for electrons can be described by the Schrödinger equation

$$\frac{\mathrm{d}^2}{\mathrm{d}z^2}\psi_i(z) + \frac{2m^*}{\hbar^2}(E_i - E_\mathrm{c}(z))\psi_i(z) = 0\,, \qquad (1)$$

where m^* is the effective electron mass, E_i and ψ_i, where $i = 0, 1, 2\cdots, N_{E_i} - 1$, are 2DEG energy levels and wavefunctions respectively, and N_{E_i} is the number of 2DEG energy levels. The conduction band edge satisfies $E_\mathrm{c}\,(z) = -eV(z) + \Delta E_\mathrm{c}(z)$, where $V(z)$ is the electron static potential, and ΔE_c is the conduction band offset at a hetero-interface.

From Eq.(1) the 2DEG sheet density N_s2D and spatial distribution $n_\mathrm{2D}(z)$ are obtained as follows:

$$N_\mathrm{s2D} = \sum_i n_i = \sum_i \frac{m^* k_\mathrm{B} T}{\pi\hbar^2} \ln\left[1 + \exp\left(\frac{E_\mathrm{F} - E_i}{k_\mathrm{B} T}\right)\right], \qquad (2)$$

$$n_\mathrm{2D}(z) = \sum_i n_i \psi_i^*(z)\psi_i(z), \qquad (3)$$

$$\int \psi_i^*(z)\psi_i(z)\mathrm{d}z = 1, \quad i = 0, 1, 2, \cdots, N_{E_i} - 1,$$

where k_B is the Boltzmann constant.

The conduction band edge is solved by the Poisson equation,

$$\frac{\mathrm{d}^2}{\mathrm{d}z^2}V(z) = -\frac{\rho(z)}{\varepsilon_0\varepsilon(z)},$$

$$\rho(z) = e(N_\mathrm{D}^+(z) - n_\mathrm{t}(z)),$$

$$n_\mathrm{t}(z) = n_\mathrm{2D}(z) + n_\mathrm{3D}(z). \qquad (4)$$

In Eq.(4) the ionized donor density is

$$N_\mathrm{D}^+(z) = \frac{N_\mathrm{D}}{1 + 2\mathrm{e}^{(E_\mathrm{F} - E_\mathrm{c} + E_\mathrm{d})/(k_\mathrm{B} T)}}, \qquad (5)$$

where E_d is the donor ionization energy.

The bulk electron density obeys the Fermi distribution,

$$n_\mathrm{3D}(z) = N_\mathrm{c} F_{1/2}\left(\frac{E_\mathrm{F} - E_\mathrm{c}(z)}{k_\mathrm{B} T}\right), \qquad (6)$$

where N_c is the effective state density and $F_{1/2}$ is the half-order Fermi integral. The 2DEG and bulk electrons are differentiated with respect to energy, and there exists a natural criterion that if the difference between two adjacent energy levels is less than $k_\mathrm{B}T$, the lower will be the upper limit of 2DEG subbands and the higher will be the lower energy limit of bulk electrons.

Define $N_\mathrm{s3D} = \int n_\mathrm{3D}(z)\mathrm{d}z$ for bulk electrons, then the total electron sheet density will be $N_\mathrm{st} = N_\mathrm{s2D} + N_\mathrm{s3D}$. If the depth from the top of the structures to GaN channel is d, two ratios used in discussion below can be defined here:

$$r_\mathrm{2D} = \int_0^d n_\mathrm{2D}(z)\mathrm{d}z / N_\mathrm{s2D}$$

and

$$r_\mathrm{t} = \int_0^d n_\mathrm{t}(z)\mathrm{d}z / N_\mathrm{st}. \qquad (7)$$

Both r_2D and r_t reflect the proportion of electrons distributed in the barrier layer to that in the whole structure, but the former is for the 2DEG and the latter for the total electron density.

With the Fermi level E_F chosen as the energy reference, the boundary conditions for the Poisson equation are $E_\mathrm{c}|_{z=0} = 1.2\,\mathrm{eV}$ at the AlGaN surface and $F|_{z=z_\mathrm{max}} = 0$ at the bottom of GaN, where F is the electric field.

At the hetero-interface there exists the electric displacement continuity,

$$\varepsilon_1\varepsilon_0 F_1 + \sigma_\mathrm{pol} = \varepsilon_2\varepsilon_0 F_2, \qquad (8)$$

$$\sigma_\mathrm{pol} = P_\mathrm{PE1} - P_\mathrm{PE2} + P_\mathrm{SP1} - P_\mathrm{SP2}, \qquad (9)$$

where ε is the dielectric constant and σ_pol the sheet polar charge. The subscripts 1 and 2 are for different materials adjacent to the hetero-interface. P_PE is the piezoelectric polarization and P_SP the spontaneous polarization. The polarization effects are studied by using the nonlinear models.[3]

In the study of the effect of temperature on the electron distribution, the variations of polarization and conduction band offset are considered besides the items directly related to temperature in the equations above.

The change of the polarization effects, or exactly the change of piezoelectric polarization with temperature as a result of thermal expansion of the lattice, is described as follows:

$$P_\mathrm{PE}(\mathrm{Al}_x\mathrm{Ga}_{1-x}\mathrm{N}, \mathrm{ALN}) = f(\zeta), \quad \zeta = \frac{a_\mathrm{GaN} - a}{a}, \qquad (10)$$

$$a(T) = a_0(1 + \beta(T - T_0)), \qquad (11)$$

where a is the lattice constant of $\mathrm{Al}_x\mathrm{Ga}_{1-x}\mathrm{N}$ or AlN, and β is the thermal expansion coefficient of a. T_0 is taken as 300 K, and a_0 is the lattice constant at 300 K.

The conduction band offset changes with temperature as a result of the temperature dependence of nitride band gap,[4]

$$E_\mathrm{g} = E_{\mathrm{g}_0} - AT^2/(T + B)\ \ (\mathrm{eV}). \qquad (12)$$

In Table 1, parameters needed for Eqs.(10)–(12) are presented.

Table 1. Some basic parameters.

	a_0 /Å	$\beta/10^{-6}\mathrm{K}^{-1}$	E_{g_0} /eV	$A/10^{-4}$	B
AlN	3.112	4.20	6.23	17.99	1462
GaN	3.189	5.59	3.507	9.09	830

The self-consistent solution of the above model is similar to that in Ref.[5], and the values of the other relevant parameters are mainly cited from Ref.[6].

3. Calculations and analysis

The two structures considered here are similar to those in Ref.[1]. Structure A is $Al_{0.25}Ga_{0.75}N/GaN$, and $Al_{0.25}Ga_{0.75}N$ layer includes a 20 nm Si-doped layer and a 5 nm spacer layer without doping. The GaN layer is defined to be 300 nm in thickness without doping, and the bottom boundary is so far from the quantum well that the boundary condition of zero electric field can be adopted. Structure B is $Al_{0.25}Ga_{0.75}N/AlN/GaN$, which is formed by adding a 1 nm AlN interlayer to the AlGaN/GaN heterointerface in Structure A.

3.1. Effect of donor density

Conduction band and electron profiles at zero doping are shown in Fig.1 for both A and B structures. In Structure B as a result of the larger effective ΔE_c caused by polarization field, the quantum well is deeper, the peak electron density is higher, and especially the barrier penetration of the two-dimensional electrons is significantly lower. So alloy disorder scattering is weakened and the 2DEG mobility improved. Also elevated is the energy band in barrier layer, which will fall with the increase of donor density N_D, and the barrier parallel conduction (BPC) may eventually appear. So it is predicted that the resistance to BPC is stronger in Structure B.

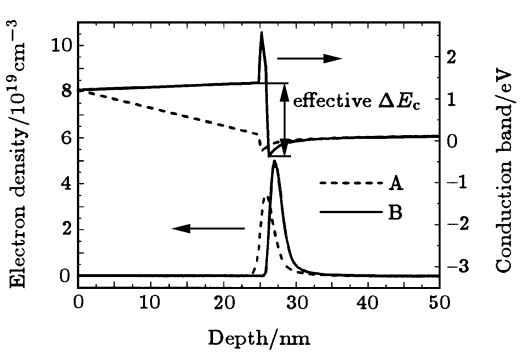


Fig.1. Distributions of conduction band E_c and electron density n_t at zero doping for Structures A and B.

Conduction band and electron profiles at $N_D=1\times10^{19}\,\mathrm{cm}^{-3}$ are shown in Fig.2(a) for both A and B structures. At the quantum well, electron density of Structure B is still higher than that of Structure A; but their difference is larger. From the electron profiles in the barrier shown in Fig.2(b), at the depth of less than 20 nm, the major component of n_t is n_{3D} for both A and B structures, which also makes the major contribution to the BPC. But n_{3D} in Structure B is far less than that in Structure A, so is the absolute BPC. Meanwhile, n_{2D} or the difference between n_t and n_{3D} is present in only AlN layer in the barrier of Structure B, but in Structure A, n_{2D} reaches a density of $10^{17}\,\mathrm{cm}^{-3}$ at the depth of less than 20 nm. So compared with zero doping, the 2DEG in Structure A spreads and experiences more ionized donor scattering and alloy disorder scattering in the barrier, and the deterioration of 2DEG mobility is larger in Structure A.

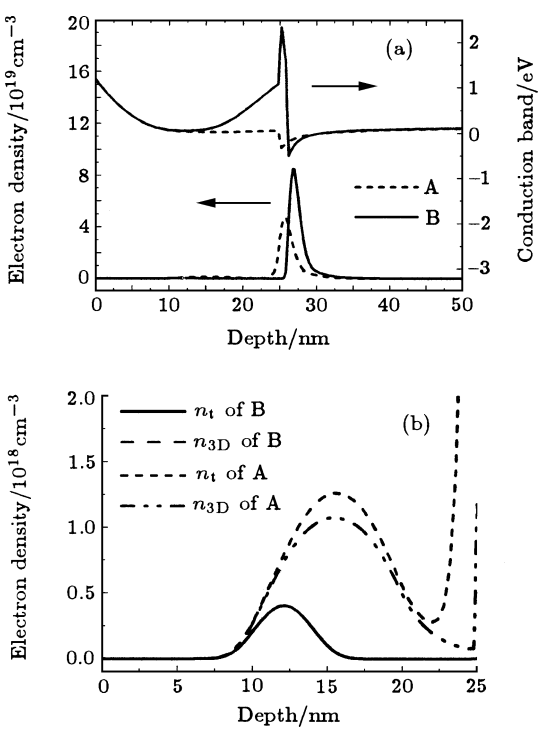


Fig.2. Distributions of E_c and n_t at a donor density $N_D=1\times10^{19}\,\mathrm{cm}^{-3}$ in the AlGaN layer for Structures A and B (a) E_c and n_t over 0–50 nm (b) Enlarged view of n_t over 0–25 nm. n_{3D} shows the composition of n_t.

Figure 3 shows the changes of some important quantities with N_D increasing. As defined in Section 2, r_{2D} is the proportion of 2DEG penetration into the barrier, and reflects the amount of 2DEG experiencing scattering present in the barrier, while the difference between r_t and r_{2D} reflects the BPC effect. In the considered range of donor density, r_t is determined by r_{2D} for both the structures. r_{2D} is quite high in

Structure A, and it rises all along with N_D except for a fall at 6×10^{18}–$7\times10^{18}\,cm^{-3}$, meanwhile the difference between r_t and r_{2D} grows fast. But in Structure B, r_t and r_{2D} are low (< 3%), with little change. So in the considered range of donor density, the 2DEG mobility deteriorates faster in Structure A, and BPC can be omitted in Structure B but must be taken into account in Structure A.

Also shown in Fig.3 are the 2DEG sheet density N_{s2D} and the total sheet density N_{st}. In both the structures the major component of N_{st} is N_{s2D}. When N_D is less than $3\times10^{18}\,cm^{-3}$, N_{st} curves of Structures A and B rise at the same rate. When N_D increases from $3\times10^{18}\,cm^{-3}$ to $6\times10^{18}\,cm^{-3}$, N_{st} of Structure A rises slowly. When N_D is more than $6\times10^{18}\,cm^{-3}$, N_{st} in Structure A still rises but N_{s2D} starts to fall. r_t and r_{2D} are affected at this donor density and change from rise to fall.

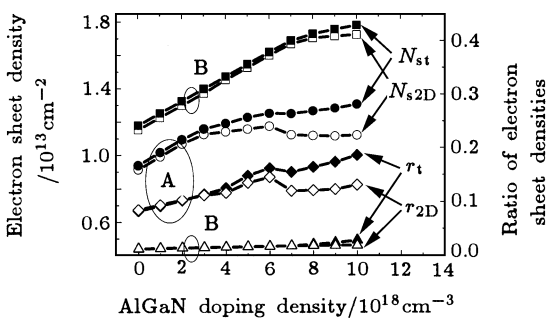


Fig.3. Total electron sheet density N_{st}, 2DEG sheet density N_{s2D}, and barrier electron proportions r_t (for the sum of 2DEG and bulk electrons) and r_{2D} (for 2DEG only) at different N_D for Structures A and B.

The explanation of such a change needs an insight into the 2DEG. The bottom energy of the quantum well E_{ch} and 2DEG energy levels are shown in Fig.4 for both the structures. The donor density $6\times10^{18}\,cm^{-3}$ is found to be a turning point for Structure A. When N_D is lower than $6\times10^{18}\,cm^{-3}$, the absolute value of E_{ch} or the depth of the quantum well increases with N_D, though such an increase is not considerable when $N_D > 3\times10^{18}\,cm^{-3}$. And there exist three 2DEG energy levels, all of which shift downward as the quantum well is deeper. When N_D is higher than $6\times10^{18}\,cm^{-3}$, the quantum well turns shallower, and the 2DEG energy levels, whose number reduces to two, shift upward. This is consistent with the decrease of N_{s2D}. A comparison between the electron densities in the barrier at N_D=$6\times10^{18}\,cm^{-3}$ and $7\times10^{18}\,cm^{-3}$ shows that n_t and n_{2D} are lower, but n_{3D} is higher for the latter.

So when N_D increases, the quantum well accumulates more and more electrons supplied by the barrier donor and the 2DEG density rises. But once the energy band depression in the barrier, caused by the increase of N_D, reaches a 'threshold', electrons start to populate the barrier as bulk electrons. The electron accumulation and confinement of the quantum well are weakened, the 2DEG density falls but bulk electron density rises, and the three-dimensional property of the whole electron system turns prominent. This is consistent with the change of r_t and r_{2D}.

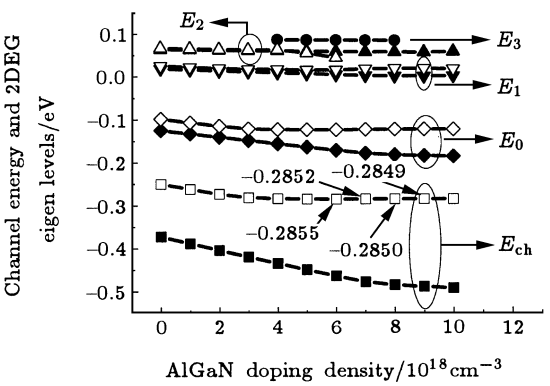


Fig.4. The lowest conduction band energy of the channel E_{ch} and 2DEG energy levels E_i at different N_D for both Structures A and B. The open-symbol lines are for Structure A and the solid-symbol lines are for Structure B.

In Structure B, N_{st} and N_{s2D} both increase in the whole range of donor density. When N_D is higher than $3\times10^{18}\,cm^{-3}$, the number of 2DEG energy levels N_{E_i} changes from 3 to 4, so the quantum well is deeper, the 2DEG energy range is larger and the electron density higher. When N_D is higher than $8\times10^{18}\,cm^{-3}$, the increase of N_{s2D} slows down and correspondingly N_{E_i} reduces from 4 to 3. So the 2DEG in Structure B is also affected by the electron population in the barrier at high donor densities, but it keeps an efficient absorption of the electrons supplied by the barrier donor.

Altogether, when donor density increases, the 2DEG in Structure B has a better stability than in Structure A. It absorbs the electrons from donor efficiently and keeps a small spatial extension, so the influence of alloy disorder scattering on its mobility is relatively weak. Moreover, the resistance to BPC is stronger in Structure B. All these result from the larger effective ΔE_c.

3.2. Effect of temperature

The calculations at different temperatures with N_D=$5\times10^{18}\,cm^{-3}$ are shown in Fig.5 and Fig.6. Fig-

ure 5 presents r_{2D}, r_t, N_{s2D} and N_{st}. Figure 6 presents E_{ch} and 2DEG energy levels. As for the effect of temperature on 2DEG in nitride hetero-structures, some relevant studies have been carried out.[7] The similar model here gives the similar results, which reflect the commonness in the temperature dependence of electron systems in the two structures. As temperature rises, band gaps become smaller, so are conduction band offsets at hetero-interfaces. The quantum well is shallower as shown by E_{ch} in Fig.6, and the 2DEG density decreases. The strain is larger because of thermal expansion of the lattice, which alleviates the above tendency partially. The bulk electron density increases with temperature for N_c is proportional to $T^{2/3}$. But it is noted that the 2DEG stabilities are different between Structures A and B.

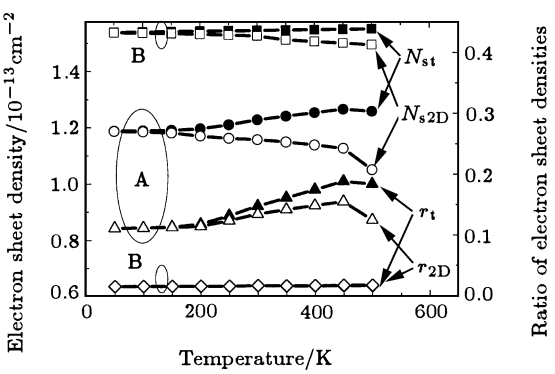


Fig.5. N_{st}, N_{s2D}, r_t and r_{2D} at different temperatures for Structures A and B.

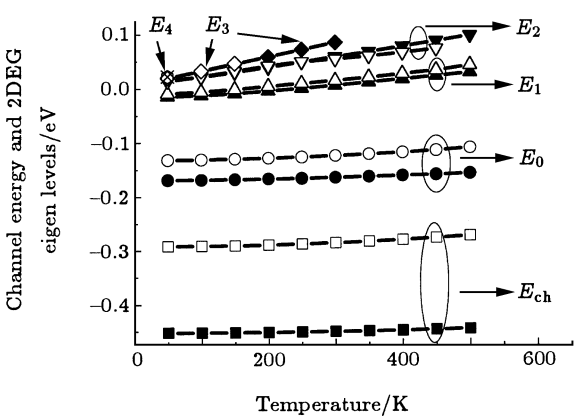


Fig.6. E_{ch} and E_i at different N_D for both Structures A and B. The open-symbol lines are for Structure A and the solid-symbol lines are for Structure B.

In Structure A, the number of 2DEG energy levels N_{E_i} reduces gradually from 5 at 50 K to 2 at 500 K, and the reduction rate of N_{s2D} becomes larger at the temperatures where N_{E_i} changes. When N_{E_i} changes from 50 K to 100 K and from 150 K to 200 K, N_{E_i} reduces as a result of shallower quantum well. But r_{2D} and r_t are equal in the former case while different in the latter case, implying the presence of bulk electrons in the barrier. Figure 7 presents the electron densities in the barrier at different temperatures. Bulk electrons do appear as the major part of n_t at the depths of 15 nm–20 nm from 150 K to 200 K, though the density is low (10^{17} cm^{-3} at 200 K). From 200 K to 450 K, thermal activation of carriers is enhanced. Though N_{E_i} stays constant, smaller ΔE_c and shallower quantum well result in more penetration of 2DEG into the barrier, thus r_{2D} increases. The bulk electron density grows higher throughout the structure, and the difference between r_t and r_{2D} is larger. The changes of N_{s2D} and r_{2D} are greatest from 450 K to 500 K, and in the barrier n_t and n_{2D} are lower, but n_{3D} is higher.

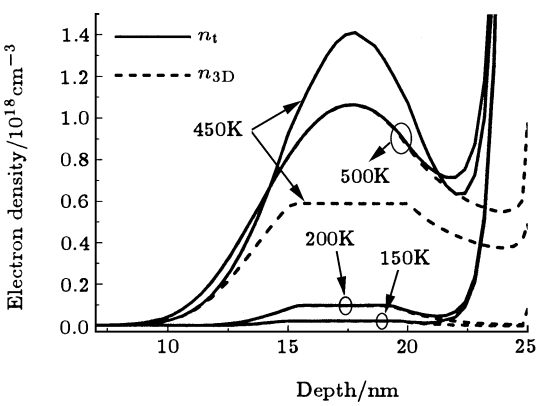


Fig.7. n_t in the barrier of Structure A at the temperatures where the number of 2DEG energy levels changes. n_{3D} shows the composition of n_t.

While in Structure B, N_{E_i} changes from 4 to 3 at 300 K only, the reduction rate of N_{s2D} is larger at this temperature, but smaller than that of Structure A when T >150 K (also the temperature where N_{E_i} changes from 4 to 3). r_t and r_{2D} stay below 2% all along, which implies neglectable barrier penetration of 2DEG and the absence of BPC.

So the influence of bulk electrons is greater, the penetration of 2DEG into the barrier is larger and the BPC is more easily activated thermally in Structure A. Correspondingly, the two-dimensional property of the electron system is more prominent in Structure B and the 2DEG stability is also higher in Structure B in the considered temperature range, which should also be ascribed to the larger effective ΔE_c.

4. Experimental results

The reported experimental results of parallel conduction in the GaN-based structures are mostly involved with the magnetic-field-dependent or

temperature-dependent Hall effects.[8] In these experiments the spatial distribution of the parallel conduction cannot be determined. While a widely-used simple method to show the carrier density vs depth profile in a semiconductor hetero-structure is the Schottky $C-V$ characteristics,[9] which is chosen to test our calculations. And only the effect of temperature is evaluated.

From some published Hall data of GaN-based hetero-structures,[10,11] the Hall electron density rises with temperature, so the total electron density is higher. Based on the above calculations, when temperature is higher, the 2DEG density will be lower, the electron density for parallel conduction will be higher. And the structure with a higher 2DEG density at room temperature will show a lower temperature-activated parallel conduction or electron density outside the channel.

Two hetero-structure samples of Structures A and B are grown on sapphire by the MOCVD technique, and they are made Schottky diodes. For the diodes the Schottky contact is a circle with a diameter of 120μm, and the ohmic contact is the ring concentric with the circle. The details of material growing and diode processing are similar to those in Ref.[12]. The $C-V$ characteristics are measured at 100 kHz by Keithley 590 $C-V$ analyser. A Westbond K1200D hot plate is used to heat the samples. The temperature ranges from 293.5 K to 473.5 K with 25 K/step above 323.5 K.

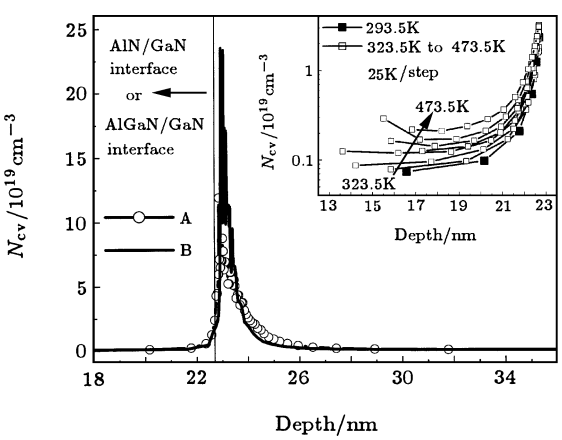


Fig.8. The $C-V$ carrier density profiles at 293.5K for two diodes on Structures A and B respectively. The hetero-interface is set at 22.7 nm in depth. The inset shows the change of the carrier distribution in the barrier layer with temperature for Structure A.

Figure 8 shows the carrier density profiles of two diodes on Structures A and B at 293.5 K. The carrier density peaks at almost the same depth, but the peak density is higher in Structure B. The difference between peak densities agrees with an early observation of Hg-probe.[13] For a convenient comparison between Structures A and B, the AlN/GaN interface for Structure B and AlGaN/GaN interface for Structure A are both set at 22.7 nm in depth. The inset shows the carrier distribution in the barrier layer at different temperatures for Structure A, and it is obvious that the carrier density increases with temperature. The similar tendency is observed in Structure B.

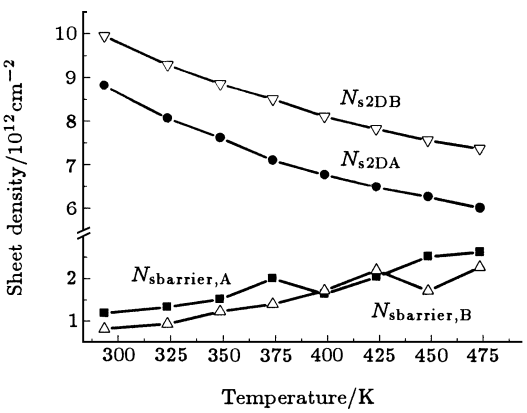


Fig.9. The temperature-dependent carrier sheet density integrated by N_{cv} profiles. N_{s2D} is integrated from 22.7 nm to 26 nm in depth, and $N_{sbarrier}$ is from the detectable depth in the barrier layer to 22.7 nm.

To compare with the calculations shown in Fig.5, a rough evaluation is taken by integrating N_{cv} profiles for the measured N_{s2D} from 22.7 nm to 26 nm in depth, and for $N_{sbarrier}$ from the detectable depth in the barrier layer to 22.7 nm. The results are shown in Fig.9. For both the structures, N_{s2D} falls but $N_{sbarrier}$ rises. While in the considered temperature range N_{s2DB} is always higher than N_{s2DA}, and their difference increases from $1.1389\times10^{12}\,cm^{-2}$ at 293.5 K to $1.3636\times10^{12}\,cm^{-2}$ at 473.5 K. And in spite of the fluctuation of $N_{sbarrier}$ caused by the change of the detectable depth in the barrier layer with temperature, generally $N_{sbarrier,B}$ is lower than $N_{sbarrier,A}$. All these are in good agreement with our calculations, and show the thermally activated parallel conduction.

5. Conclusions

In nitride-based hetero-structures, increasing the donor density in the barrier layer helps enhance the 2DEG density, but it makes possible the presence of barrier parallel conduction. The thermal activation of carriers, as temperature increases, enhances the three-dimensional property of the whole electron system, and the 2DEG degenerates. The self-consistent solv-

ing of one-dimensional Schrödinger–Poisson equations is carried out to investigate the electron systems in AlGaN/AlN/GaN and AlGaN/GaN structures from the points of view of increasing both donor density and temperature. It is revealed that as a result of larger effective ΔE_c, in the former structure the quantum well is deeper and the energy band in the barrier is higher. So the 2DEG absorbs the electrons from donor ionization/thermal activation efficiently in quite a large range of donor density/temperature, keeps high electron density and small spatial extension, and thus 2DEG mobility deteriorates more slowly. Meanwhile, the AlGaN/AlN/GaN structure features stronger resistance to barrier parallel conduction. The $C - V$ carrier density profiles are measured at different temperatures for two considered structures and present an experimental proof for our calculations.

References

[1] Shen L, Heikman S, Moran B, Coffie R, Zhang N Q, Buttari D, Smorchkova I P, Keller S, DenBaars S P and Mishra U K 2001 *IEEE Electron Dev. Lett.* **22** 457

[2] Smorchkova I P, Chen L, Mates T, Shen L, Heikman S, Moran B, Keller S, DenBaars S P, Speck J S and Mishra U K 2001 *J. Appl. Phys.* **90** 196

[3] Fiorentini V, Bernardini F and Ambacher O 2002 *Appl. Phys. Lett.* **80** 1204

[4] Vurgaftman I, Meyer J R and Ram-Mohan L R 2001 *J. Appl. Phys.* **89** 5815

[5] Tan I H, Snider G L, Chang L D and Hu E L 1990 *J. Appl. Phys.* **68** 4071

[6] Ambacher O, Smart J, Shealy J R, Weimann N G, Chu K, Murphy M, Schaff W J, Eastman L F, Dimitrov R, Wittmer L, Stutzmann M, Rieger W and Hilsenbeck J 1999 *J. Appl. Phys.* **85** 3222

[7] Zhang J F, Zhang J C and Hao Y 2004 *Chin. Phys.* **13** 1334

[8] Dziuba Z, Antoszewski J, Dell J M, Faraone L, Kozodoy P, Keller S, Keller B, DenBaars S P and Mishra U K 1997 *J. Appl. Phys.* **82** 2996

[9] Zhong Y G, Shen B, Liu J, Yu H Q, Zhou H M, Qian Y, Zhang R, Shi Y and Zheng Y D 2001 *Chin. J. Semiconductors* **22** 1420 (in Chinese)

[10] Arulkumaran S, Egawa T, Ishikawa H and Jimbo T 2002 *Appl. Phys. Lett.* **80** 2186

[11] Gökden S 2003 *Turk. J. Phys.* **27** 205

[12] Zhang J C, Wang C, Yang Y, Zhang J F, Feng Q, Li P X and Hao Y 2005 *Chin. J. Semiconductors* **26** 2396 (in Chinese)

[13] Zhang J C 2003 *Growth of AlGaN/GaN Heterostructures and Fabrication of High Electron Mobility Transistors* Ph. D. Thesis of Xidian University p75 (in Chinese)